First Examples of β-Diketonate Platinum(II) Complexes with Sulfoxide Ligands

Sandra A. De Pascali,[a] Paride Papadia,[a] Antonella Ciccarese,[a] Concetta Pacifico,[b] and Francesco P. Fanizzi*[a]

Keywords: Platinum / β-Diketonate / S ligands

New platinum(II) complexes have been prepared as models for explaining the coordination of multiple β-diketonate ligands to give [Pt(*O,O′*-acac)(γ-acac)L] species. The new compounds containing both an *O,O′*-chelated acetylacetonate ligand and a sulfoxide in the platinum coordination sphere, [PtCl(*O,O′*-acac)(DMSO)] (**1**) and [Pt(*O,O′*-acac)(γ-acac)(DMSO)] (**2**), have been synthesised and characterised by ^{1}H, ^{13}C, ^{195}Pt 1-D and 2-D NMR heteronuclear correlation spectroscopy and, in the case of **2**, by X-ray crystal structure analysis also. Moreover, a new synthetic pathway to obtain the previously reported complex K[Pt(*O,O′*-acac)(γ-acac)$_2$] (**3**) has been developed. The data presented herein are consistent with a reaction mechanism which explains the subsequent steps of the coordination of multiple β-diketonate ligands to platinum(II) complexes, where the first species formed contains one *O,O′*-chelated acac group.

Introduction

Despite the fact that sulfoxides[1,2] and acetylacetone[3] have been widely used in the coordination and organometallic chemistry of platinum, to the best of our knowledge, no platinum(II) complexes containing both ligands have been described so far. In particular, platinum(II) shows a high affinity for sulfur ligands, a large number of complexes with sulfoxides are known and several studies of DMSO complexes dealing with a wide variety of different aspects of these complexes have been carried out.[4] On the other hand, the versatility of acetylacetone as a ligand was first demonstrated by Werner who employed it as a chelating agent.[5] Almost every metal has been found to give acetylacetone complexes which, in many cases, have exhibited interesting stereochemical arrangements. Several reports on acetylacetonatoplatinum(II) complexes have established the presence of two main modes of metal-ligand bonding: oxygen-bonded (chelated) acetylacetonate and carbon-bonded acetylacetonate.[6–9] In many cases, two acetylacetonate (acac) ligands, one of them oxygen-bonded (*O,O′*-chelated) and the other one carbon-bonded (σ-bonded), are coordinated to the same metal centre. Very extensive studies have been performed on the reactions of bis(β-diketonato)palladium(II) and platinum(II) complexes of the type [M(*O,O′*-acac)$_2$] (M = Pd or Pt, *O,O′*-acac = *O,O′*-acetylacetonate) with nitrogen ligands (py and Et_2NH), tertiary phosphanes (PPh_3, PCy_3 and PEt_3) and arsines which resulted in the bonding mode conversion for at least one *O,O′*-chelated β-diketonate anion to other type of coordination modes.[10,11] It was found that the addition of a series of ligands (L) to [Pt(*O,O′*-acac)$_2$] caused the rearrangement of one of the *O,O′*-chelated acac ligands to a σ-bonded form, affording complexes of the type [Pt(*O,O′*-acac)(γ-acac)L] (γ-acac = Cγ-bonded acetylacetonate).[12] The reaction of [Pt(*O,O′*-acac)$_2$] with an excess of pyridine, on the other hand, yielded a complex in which both acetylacetonate ligands are coordinated to platinum through the central carbon atoms, [Pt(γ-acac)$_2$(py)$_2$], in equilibrium with a mono-γ-acac complex, [Pt(*O,O′*-acac)(γ-acac)(py)].[13] Interestingly, reactions giving [Pt(*O,O′*-acac)(γ-acac)L] complexes starting from platinum species other than [Pt(*O,O′*-acac)$_2$] and, in general, lacking an acac ligand previously bound to the metal, appear to be much less common. Representative examples for this latter kind of reaction are the syntheses of K[Pt(*O,O′*-acac)(γ-acac)Cl][6] and [Pt(*O,O′*-acac)(γ-acac)-(Et_2S)][14] starting from $K_2[PtCl_4]$ and [$PtCl_2(Et_2S)_2$], respectively. Furthermore, the subsequent coordination of two acac ligands in the reactions of [$PtCl_2L_2$]-type complexes [L = Et_2S, 1,2-bis(ethylthio)ethane, PEt_3, PPh_3] with thallium(I) β-diketonates has been examined (Scheme 1). The factors favouring each of the two coordination modes, *O,O′*-chelated or Cγ-bonded, when the first acac binds the metal were investigated but no definitive conclusions were drawn about the pathway leading to [Pt(*O,O′*-acac)(γ-acac)-L] complexes.[14]

[a] Dipartimento di Scienze e Tecnologie Biologiche ed Ambientali, Università di Lecce,
Prov.le Monteroni/Lecce, 73100 Lecce, Italy
[b] Dipartimento Farmaco-Chimico, Università di Bari,
Via E. Orabona 4, 70125 Bari, Italy
Fax: (internat.) +39-(0)832-298626
E-mail: fp.fanizzi@unile.it
Supporting information for this article is available on the WWW under http://www.eurjic.org or from the author.

  DOI: 10.1002/ejic.200400665

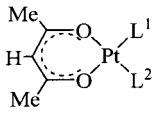

$L^1 = L^2 = \gamma$-acac, Cl, Et_2NH, PPh_3, PEt_3, piperidine
L^1 = Cl; $L^2 = PEt_3$

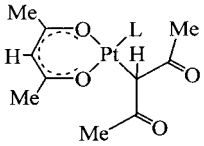

L = Cl, Et_2NH, Et_2S, PCy_3, PPh_3, Py

Scheme 1

In this context, we have synthesised two novel complexes of platinum(II), namely [PtCl(*O,O′*-acac)(DMSO)] (**1**) and [Pt(*O,O′*-acac)(γ-acac)(DMSO)] (**2**), as models for explaining the coordination of multiple β-diketonate ligands to give [Pt(*O,O′*-acac)(γ-acac)L] species. Together with the synthesis and characterisation of the new complexes **1** and **2**, we also report herein a new synthetic pathway for the homoleptic complex K[Pt(*O,O′*-acac)(γ-acac)$_2$] (**3**), previously obtained by Lewis et al.[6] Compounds **1**–**3** (Scheme 2) have been characterised by microanalysis, IR spectroscopy, multinuclear multidimensional NMR spectroscopy and, in the case of **2**, by X-ray diffraction.

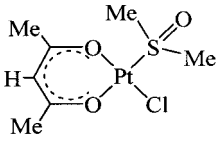

1

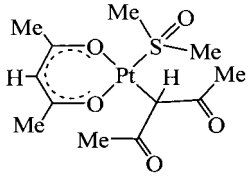

2

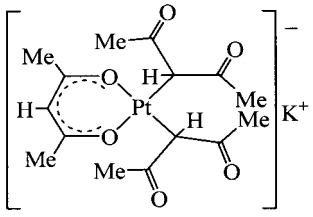

3

Scheme 2

Results and Discussion

Synthesis of the Compounds

The synthesis of [PtCl(*O,O′*-acac)(DMSO)] (**1**), containing a single chelate acac, was straightforward since, due to its low solubility in the reaction medium, it precipitates as a pale yellow powder from the reaction mixture of K[$PtCl_3$(DMSO)] with acetylacetone and KOH in water. Complexes **2** and **3** were obtained by treating [$PtCl_2(DMSO)_2$] with acetylacetone and KOH in MeOH and were isolated from their respective reaction mixtures by an appropriate workup procedure reported in the experimental section. In all cases, in order to prevent metal reduction, a slight excess of acetylacetone was used with respect to the calculated stoichiometric amount of KOH based on starting platinum complex. It should be noted that the use of the scarcely soluble [$PtCl_2(DMSO)_2$] as a starting platinum complex for the preparation of **1** in MeOH or water gave unsatisfactory results. Due to the low solubility of [$PtCl_2(DMSO)_2$], the reaction with acetylacetone and KOH in MeOH resulted in an excess of acac in solution, even when using a stoichiometric or substoichiometric amount of acac and always gave a mixture of **1**, **2** and unreacted starting material. On the other hand, the reaction of [$PtCl_2(DMSO)_2$] with acetylacetone and KOH in water, in which both the starting platinum complex and [PtCl(*O,O′*-acac)(DMSO)] are sparingly soluble, gave analytically pure **1** although a longer reaction time was required and a lower yield was obtained. Quadrangular, pale-yellow X-ray quality crystals of [Pt(*O,O′*-acac)(γ-acac)(DMSO)] (**2**) were obtained from a $CHCl_3$/pentane solution.

Characterisation of the Complexes

All complexes were characterised by microanalysis, IR spectroscopy and multinuclear, multidimensional NMR spectroscopy. In the case of compound **2**, the structure assigned on the basis of spectroscopic and microanalytical data was also confirmed by a single-crystal X-ray diffraction analysis. ^{1}H, ^{13}C NMR and ^{195}Pt NMR spectroscopic data are reported in Table 1, Table 2 and Table 3, respectively. Crystal data, data collection and refinement parameters for compound **2** are summarised in Table 4 and Table 5.

In the IR spectrum of complex **1**, the observed stretching frequencies for Cγ-H (above 3000 cm^{-1}), C=C (1570 cm^{-1}) and C=O (1520 cm^{-1}) were indicative of acetylacetonate bonded through oxygen. For chelate acetylacetonate complexes, the highest reported stretching frequencies for C=O are below 1600 cm^{-1}, in agreement with the "aromatic" nature of the system resulting from delocalization of the π elec-

Table 1. ^{1}H NMR spectroscopic data (δ) for acac ligands and complexes; * values of $J_{H\text{-}Pt}$ [in brackets] are given when assignable; # indicates the acac methyl group *cis* to DMSO

	Solvent	H/Cγ	Me/acac	Me/DMSO
acac	$CDCl_3$	5.46, 3.55	2.01, 2.20	
	CD_3OD	5.60	2.01, 2.18	
1	$CDCl_3$	5.56	2.02#, 2.06	3.44[40]*
2	$CDCl_3$	5.53(O-bonded)	1.95#, 2.01 (O-bonded)	3.31[40]
		4.80[120] (Cγ-bonded)	2.29[5] (Cγ-bonded)	
3	CD_3OD	5.39 (O-bonded)	1.77 (O-bonded)	
		4.75[120] (Cγ-bonded)	2.18 (Cγ-bonded)	
	D_2O	5.45 (O-bonded)	1.71 (O-bonded)	
		4.70[110] (Cγ-bonded)	2.07 (Cγ-bonded)	

Table 2. ^{13}C NMR spectroscopic data (δ) of complexes; * values of $J_{H\text{-}Pt}$ [in brackets] are given when assignable; # indicates the acac methyl group *cis* to DMSO

	Solvent	C/Cγ	C/Me(acac)	C/Me(DMSO)	C/C=O
1	$CDCl_3$	102.27[73]*	26.31	44.26[56]	185.87[16] 185.06#[28]
2	$CDCl_3$	102.19[64] (O-bonded) 42.04[652] (Cγ-bonded)	27.54, 27.28# (O-bonded) 30.94[125] (Cγ-bonded)	42.95[56]	185.79#, 184.93 (O-bonded) 208.53[60] (Cγ-bonded)
3	CD_3OD	101.97 (O-bonded) 44.00 (Cγ-bonded)	27.95 (O-bonded) 30.16 (Cγ-bonded)		184.58 (O-bonded) 211.55 (Cγ-bonded)
	D_2O	101.66 (O-bonded) 43.08 (Cγ-bonded)	27.52 (O-bonded) 29.75 (Cγ-bonded)		185.76 (O-bonded) 212.69 (Cγ-bonded)

Table 3. ^{195}Pt NMR spectroscopic data (δ) of complexes

	Solvent	
1	$CDCl_3$	–2399
	CD_3OD	–2430
2	$CDCl_3$	–3198
	CD_3OD	–3168
3	CD_3OD	–2539
	D_2O	–2555

Table 4. Crystallographic data and structure refinement of complex **2**

Empirical formula	$C_{12}H_{20}O_5PtS$
Formula mass	1414.29
Temperature	293(2) K
Wavelength	0.71069 Å
Crystal system, space group	triclinic, $P\bar{1}$
Unit cell dimensions	a = 9.439(5) Å, α = 74.488(5)° b = 13.237(5) Å, β = 91.336(5)° c = 21.026(5) Å, γ = 107.607(5)°
Volume	2408.0(17) Å^3
Z, Calculated density	6, 1.951 gcm^{-3}
Absorption coefficient	8.881 mm^{-1}
F(000)	1356
θ range for data collection	1.01 to 23.25°
Limiting indices	$-10 \le h \le 10$, $-13 \le k \le 14$, $0 \le l \le 23$
Reflections collected/unique	6726/6726 [R(int) = 0.0170]
Completeness to θ = 23.25°	97.1%
Refinement method	Full-matrix least-squares on F^2
Data/restraints/parameters	6726/0/533
Goodness-of-fit on F^2	1.060
Final R indices [$I > 2\sigma(I)$]	R_1 = 0.0393, wR_2 = 0.1163
R indices (all data)	R_1 = 0.0401, wR_2 = 0.1171
Largest diff. peak/hole	1.376/–0.855 e·Å^{-3}

Table 5. Selected bond lengths [Å] and angles [°] in complex **2** (three independent molecules *2*, *2a*, and *2b*)

	2	*2a*	*2b*
Pt(1)–O(2)	2.009(6)	2.000(5)	2.003(6)
Pt(1)–O(1)	2.045(5)	2.061(5)	2.062(6)
Pt(1)–C(8)	2.095(8)	2.096(8)	2.077(9)
Pt(1)–S(1)	2.188(2)	2.186(2)	2.177(2)
S(1)–O(5)	1.47(1)	1.46(1)	1.44(1)
S(1)–C(12)	1.75(1)	1.77(1)	1.75(1)
S(1)–C(11)	1.79(1)	1.77(1)	1.76(1)
O(1)–C(2)	1.28(1)	1.29(1)	1.29(1)
O(3)–C(7)	1.21(1)	1.23(1)	1.26(1)
O(2)–C(4)	1.27(1)	1.29(1)	1.23(1)
O(4)–C(9)	1.23(1)	1.20(1)	1.20(1)
C(2)–C(3)	1.39(1)	1.37(1)	1.37(2)
C(3)–C(4)	1.34(1)	1.37(1)	1.36(2)
O(2)–Pt(1)–O(1)	91.7(2)	91.6(2)	91.1(3)
O(2)–Pt(1)–C(8)	88.0(3)	88.0(3)	88.1(3)
O(1)–Pt(1)–C(8)	178.2(3)	177.5(3)	179.0(3)
O(2)–Pt(1)–S(1)	176.5(2)	175.8(2)	178.6(2)
O(1)–Pt(1)–S(1)	90.9(2)	92.3(2)	90.4(2)
C(8)–Pt(1)–S(1)	89.4(2)	88.1(2)	90.5(3)
O(5)–S(1)–C(12)	108.4(5)	108.5(5)	107.4(6)
O(5)–S(1)–C(11)	108.4(5)	109.1(5)	107.5(7)
C(12)–S(1)–C(11)	101.3(5)	100.6(5)	100.8(6)
O(5)–S(1)–Pt(1)	115.2(3)	115.7(3)	119.4(4)
C(12)–S(1)–Pt(1)	111.2(4)	112.1(4)	111.2(4)
C(11)–S(1)–Pt(1)	111.4(3)	109.7(3)	108.8(4)

trons in the chelate ring.[7] The IR spectra of **2** and **3**, containing both oxygen-bonded and carbon-bonded acetylacetonate show two sets of absorptions in the C–H stretching region. The IR band above 3000 cm^{-1} was assigned to the Cγ-H vibration of the oxygen-bonded ligand whereas below 3000 cm^{-1}, both CH_3 and Cγ-H absorptions for the σ-bonded acac could be clearly identified. The high frequencies (1680–1630 cm^{-1}) of the C=O stretching modes observed in complexes **2** and **3** are further evidence that the carbonyl groups do not interact with platinum and strongly suggest that the complexes also contain a σ-bonded acac.

The absorption band at 1030 cm^{-1} in the IR spectra of **1** and **2** was assigned to the S=O stretching mode of the DMSO moiety whereas the band at 340 cm^{-1}, unique to the only new chloride complex here reported, was unambiguously attributed to the Pt–Cl stretching mode.

The ^1H NMR spectrum of **1** in $CDCl_3$ shows two singlets at δ = 2.02 and 2.06 ppm for the two methyl groups of the oxygen-bonded acetylacetonate, one singlet at δ = 5.56 ppm relative to the Cγ-H of acac and one singlet at δ = 3.44 ppm with a characteristic $^3J_{H-Pt}$ of 40 Hz for the methyl protons of the DMSO ligand. The resonance pattern is in agreement with an asymmetric *O,O′*-chelated complex which also shows the expected remarkable deshielding of the methyne proton (Cγ-H) due to the aromatic character of the metallacycle. The ^1H NMR spectrum of complex **2** in $CDCl_3$ shows a signal pattern very similar to that observed for compound **1** with only two extra resonances, i.e. one singlet at δ = 2.29 ppm ($^4J_{H-Pt}$ = 5 Hz) and one strongly ^{195}Pt-coupled singlet at δ = 4.80 ppm ($^2J_{H-Pt}$ = 120 Hz) account-

ing for six protons and one proton, respectively. The occurrence of the same signal pattern observed for complex **1** also suggests, for complex **2**, the presence of one asymmetric *O,O′*-chelated acac in the platinum coordination sphere (two methyl groups, δ = 2.01 and 1.95 ppm, one Cγ-H proton, δ = 5.53 ppm) and one coordinated DMSO (δ = 3.31 ppm, $^3J_{H-Pt}$ = 40 Hz). The observed two extra signals could be easily assigned to an extra σ-bonded acac, which occupies the fourth square-planar coordination site, on the basis of both the large platinum coupling for the Cγ-H proton at δ = 4.80 ppm and the equivalence of the methyl groups (one singlet at δ = 2.29 ppm). In both **1** and **2**, the two methyl resonances of the asymmetric *O,O′*-chelated acac were assigned to the appropriate halves of the diketonate on the basis of the NOESY cross peaks originating from the interaction of one of them with the *cis*-DMSO ligand observed in the NOESY spectra.

The ^{1}H NMR spectrum of **3** in CD_3OD consists of only four resonances at 1.77, 2.18, 4.75 and 5.39 ppm accounting for six protons, twelve protons, two protons and one proton, respectively. None of the observed signals show ^{195}Pt satellites assignable to coordinated DMSO. On the other hand, the strong ^{195}Pt coupling exhibited by the resonance at δ = 4.75 ppm ($^2J_{H-Pt}$ = 120 Hz) together with proton integration data indicate the presence of two equivalent Cγ-H protons characterised by a $^2J_{H-Pt}$ of 120 Hz and, therefore, two equivalent Cγ-bonded acac groups in the platinum coordination sphere. Two equivalent Cγ-coordinated acac moieties also account for the twelve protons resonating at δ = 2.18 ppm. The other two resonances at δ = 1.77 and 5.39 ppm in the spectrum of **3** were assigned to one symmetric *O,O′*-chelate acac ligand coordinated to the metal. Consistently, the $^2J_{H-Pt}$ values observed for the single and the two equivalent Cγ-bonded acac groups of complexes **2** and **3**, respectively, are very similar due to the presence, in both cases, of an *O,O′*-chelated acac group in the *trans* position.

The ^{13}C NMR spectra of complexes **1**–**3** confirmed the structures assigned on the basis of ^{1}H NMR spectroscopic data. One bond and long range 2-D ^{1}H-^{13}C HETCOR experiments (spectra of **2** in Figure 1) allowed correct assignments for all the ^{13}C resonances. In particular, *O,O′*-chelated and Cγ-bonded acac groups show, for the Cγ atom, very different chemical shifts and ^{195}Pt couplings. The pseudo aromatic Cγ carbons of the acac chelates resonate downfield and with much smaller ^{195}Pt coupling constants (δ = 102.27 ppm, $^3J_{C-Pt}$ = 73 Hz; δ = 102.19 ppm, $^3J_{C-Pt}$ = 64 Hz; δ = 101.97 ppm, for **1**, **2** and **3**, respectively) with respect to the corresponding carbon in the σ-bonded acac (δ = 42.04 ppm, $^1J_{C-Pt}$ = 652; δ = 44.00 ppm, for **2** and **3**, respectively). Carbonyls of the acac chelate involved in the pseudo aromatic metallacycle resonate upfield with respect to those of σ-bonded acac. The long range 2-D ^{1}H-^{13}C HETCOR spectra of **1** and **2**, together with the above mentioned NOESY data, were used to correlate the carbonyls and the methyl groups belonging to the same half of the asymmetric chelate acac. In the case of complex **1**, the two carbonyl resonances observed at δ = 185.06 and 185.87 ppm show $^2J_{C-Pt}$ values of 28 and 16 Hz, respectively, in agreement with the higher *trans* effect exhibited by DMSO compared with that of the chloro ligand.

Interestingly, in the ^{1}H-^{13}C HETCOR spectrum of **2** (in which the Cγ-bonded acac and DMSO are both coordinated to platinum), the positions of the observed cross peaks due to the coupling with the magnetically active spectator nucleus (^{195}Pt) correlate with the number of bonds

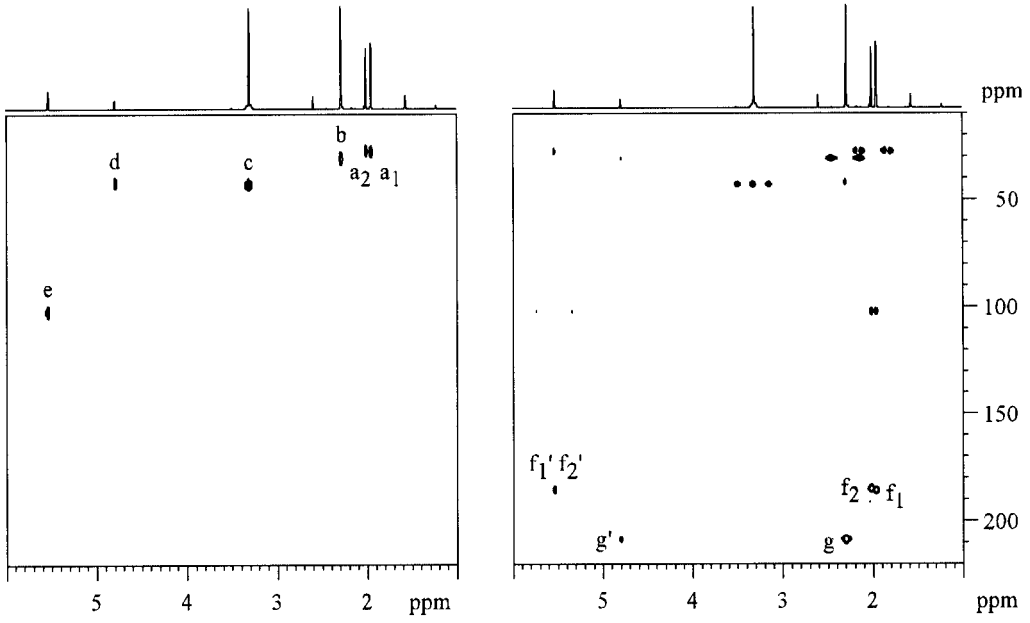

Figure 1. ^{1}H-^{13}C HETCOR (left) and ^{1}H-^{13}C long range HETCOR (right) spectra of **2**. Hydrogen bearing carbon atoms of *O,O′*-chelated acac (a_1, a_2, and e), Cγ-bonded acac (b and d) and DMSO (c) were detected by ^{1}H-^{13}C HETCOR while the carbonyls of the *O,O′*-chelated acac and the Cγ-bonded acac could be assigned according to cross peaks with methyls (f_1, f_2, and g, respectively) or according to cross peaks with Cγ-H (f_1', f_2', and g′, respectively) in the ^{1}H-^{13}C long range HETCOR spectrum

between this latter nuclues and the observed nucleus (^{1}H). The straight line joining the ^{195}Pt cross peaks shows, in the case of the platinum bound Cγ-H acac ($^2J_{H–Pt}$ = 652 Hz) and the DMSO ligand ($^3J_{H–Pt}$ = 56 Hz), a negative and positive gradient, respectively (Figure 2).[15] Another interesting feature of the ^{195}Pt coupling exhibited by [Pt(*O,O′*-acac)(γ-acac)(DMSO)] can be shown by a 2-D ^{1}H-^{195}Pt HETCOR experiment, in which all ^{195}Pt coupled protons result in cross peaks at a single platinum chemical shift (δ = –3198 ppm in $CDCl_3$). Among all the CH_3 resonances for **2**, only the methyl groups of the σ-bonded acac exhibit small cross peaks showing a very small $J_{H–Pt}$ coupling in the ^{1}H-^{195}Pt HETCOR spectrum. This may be due to a through space interaction (Figure 3). The ^{195}Pt NMR spectroscopic data of complexes **1**–**3** are reported in Table 3. The observed ^{195}Pt chemical shifts show that in [Pt(*O,O′*-acac)(DMSO)L] complexes, the shielding effect when L = Cγ-acac is considerably higher than when L = Cl^- ($\Delta\delta$, ^{195}Pt = 738 ppm in CD_3OD), while in [Pt(*O,O′*-acac)(γ-acac)L] the shielding effect is higher when L = DMSO than when L = Cγ-acac ($\Delta\delta$, ^{195}Pt = 629 ppm in CD_3OD).

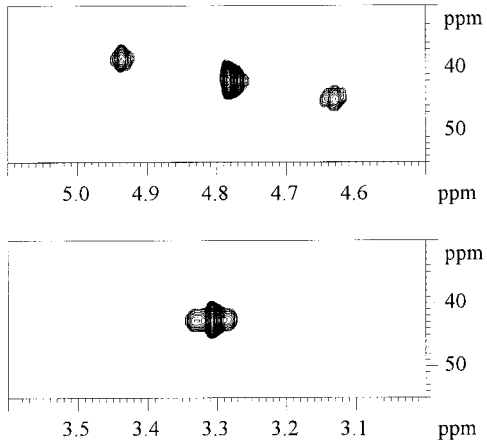

Figure 2. Expansions of ^{1}H-^{13}C HETCOR spectrum of **2** showing ^{195}Pt satellites relative to the Cγ-bonded acac (above) and the DMSO methyl groups (below)

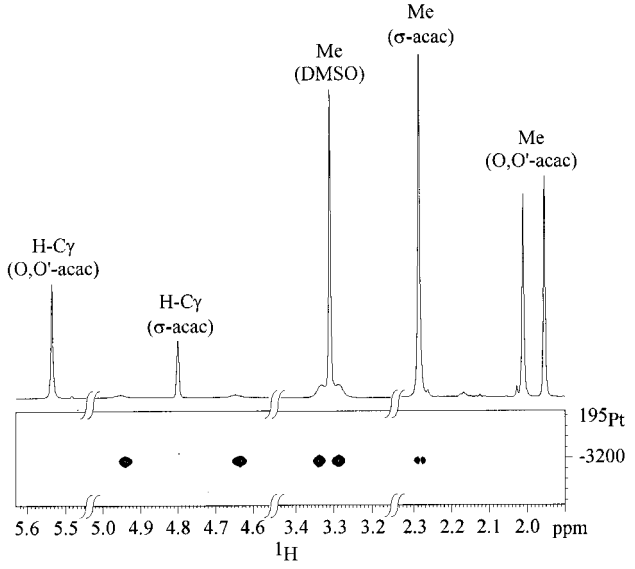

Figure 3. ^{1}H-^{195}Pt-HETCOR spectrum of **2** acquired without ^{195}Pt decoupling during acquisition. For clarity, ^{1}H projections are not on the same vertical scale

Crystal Structure of 2

The crystals obtained for complex [Pt(*O,O′*-acac)(γ-acac)(DMSO)] (Figure 4) contain three molecules in the asymmetric unit (*2*, *2a* and *2b*). The cell dimensions along with other crystallographic details are given in Table 4. In both the neutral [Pt(*O,O′*-acac)(γ-acac)(DMSO)] (**2**) and ionic [Pt(*O,O′*-acac)(γ-acac)Cl]$^-$ (**4**)[16] complexes, the oxygen-bonded acetylacetonate ligand is asymmetrically coordinated. The different Pt–O bond lengths follow the trend expected on the basis of *trans* substituents. The Pt–O lengths for the oxygen atom *trans* to the Cγ-carbon are 2.06[1] and 2.07(1) Å (square brackets indicate average values; parentheses refer to unique values) while those for the oxygen atom *trans* to the sulfur (DMSO) and chlorine atoms (complexes **2** and **4**, respectively) are 2.00[1] and 1.97(1) Å. In the σ-bonded acetylacetonate, the Pt–Cγ bond length for compound **2** is in agreement with the value for the analogous bond previously reported for **4** (2.09[2] and 2.11(2) Å, respectively). Both distances are greater than Pt–C(sp^3) σ-bonds *trans* to oxygen reported for C alkyls.[16,17] The Cγ of the σ-bonded acetylacetonate could be a weak donor, probably due to the cumulative electronegative effects of two carbonyl groups. All three *O,O′*-chelate acac moieties are planar. In all three molecules, the oxygen atoms of DMSO are oriented towards the σ-bonded acetylacetonate ligands. The modulus of the lowest torsional angles X–Pt–S–O (Ψ) (Scheme 3), according to the statistical study by Calligaris and Carugo,[2] indicates that the torsional angles Ψ lie in the low probability range [51.5(4)°, 52.4(5)° and 34.0(5)°]. This orientation of DMSO favours

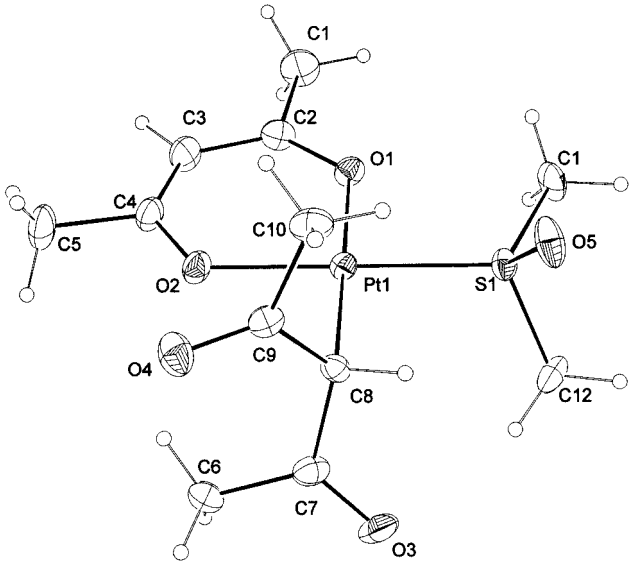

Figure 4. Molecular structure of one out of three independent molecules (molecule *2*) in the asymmetric unit of compound **2**

interactions between the oxygen atom of the DMSO and the Cγ hydrogen atom of the σ-bonded acetylacetonate [C(8)···O(5) 3.20(5), H(8)···O(5) 2.55(5) Å, C(8)···H(8)···O(5) 124(1)°].

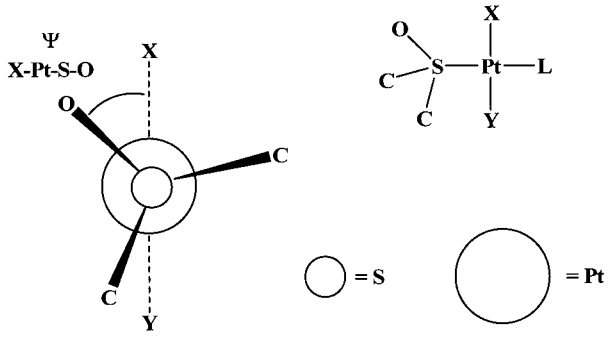

Scheme 3

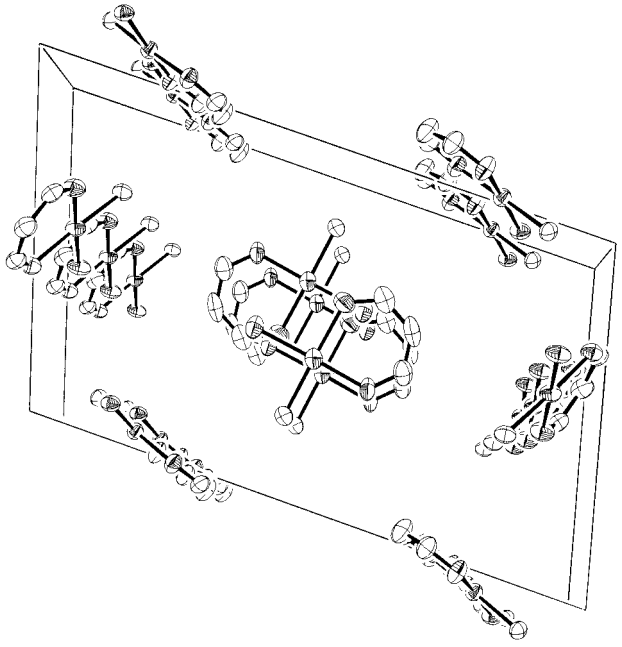

Figure 5. Unit cell projection along the *a*-axis showing alternating *2b* molecules staggered by ca. 180° and stacked inside the channel resulting from the propagation of molecules of *2* (top and bottom) and *2a* (sides). Only ligand atoms in the coordination plane are shown (see Supporting Information, S4 for the same projection with all atoms except hydrogen)

The crystal packing arrangement is shown in Figure 5. The three independent molecules of the unit cell are almost perpendicular and describe a box shape. Interestingly, the crystal structure shows subsequent boxes generating a channel by superimposition along the *a* axis. Alternating *2b* molecules are staggered by ca. 180° and stacked inside the channel created by the propagation of molecules *2* and *2a*. Selected bond distances and angles are listed in Table 5.

Reaction Mechanism

Platinum and palladium complexes of the type [M(*O,O′*-acac)(γ-acac)L] which contain one *O,O′*-chelated and one Cγ-bonded β-diketonate on the same metal together with one of a variety of nitrogen, phosphorus, arsenic and sulfur ligands (L) are well known in coordination chemistry. Usually, such complexes are produced by the addition of the ligand L to [M(*O,O′*-acac)$_2$] which causes the rearrangement of one of the two acac groups from the *O,O′*-chelate mode to the σ-bonded mode to give [M(*O,O′*-acac)(γ-acac)L] species.[12] However, in the course of our study, we have verified that treatment of the bis(β-diketonate)platinum(II) complex [Pt(*O,O′*-acac)$_2$] with excess DMSO or Et_2S[14] does not give [Pt(*O,O′*-acac)(γ-acac)L] even after two weeks. On the other hand, treatment of the starting complexes used in this work, i.e. [$PtCl_2(DMSO)_2$] and K[$PtCl_3$(DMSO)], with an excess of acetylacetone does not give [Pt(*O,O′*-acac)$_2$] in addition to [Pt(*O,O′*-acac)(γ-acac)L] and [Pt(*O,O′*-acac)(γ-acac)$_2$]$^-$. In a few cases, as for complex **2** described in this paper, [M(*O,O′*-acac)(γ-acac)L] complexes could be obtained starting from species lacking acac ligand(s) previously bound to the metal. In the case of platinum chemistry, the syntheses of K[Pt(*O,O′*-acac)(γ-acac)Cl][6] and [Pt(*O,O′*-acac)(γ-acac)(Et_2S)][14] have been reported starting from $K_2[PtCl_4]$ and [$PtCl_2$-(Et_2S)$_2$], respectively. The subsequent coordination of two acac ligands in the reactions of the [$PtCl_2L_2$]-type complexes (L = Et_2S, 1,2-bis(ethylthio)ethane, PEt_3, PPh_3) with thallium(I) β-diketonates has been studied in order to clarify the factors which could favour each of the two coordination modes, i.e. *O,O′*-chelated or Cγ-bonded, when the first acac binds to the metal. The reaction of *cis*-[$PtCl_2(PPh_3)_2$] with acac requires previous removal of the chloro ligands to give [Pt(*O,O′*-acac)(PPh_3)$_2$] while treatment of *trans*-[$PtCl_2(PEt_3)_2$] with an excess of Tl(acac) gave [Pt(*O,O′*-acac)Cl(PEt_3)]. No acetylacetonato complexes were detected in a similar reaction of *cis*-[$PtCl_2(PEt_3)_2$]. On the other hand, the reaction of *cis*- or *trans*-[$PtCl_2(Et_2S)_2$] with Tl(acac) was reported to give[Pt(*O,O′*-acac)(γ-acac)(Et_2S)] in both cases (although with different reaction rates). Interestingly, in both cases it was not possible to isolate intermediate products either by lowering the reaction temperature or by decreasing the acac/platinum complex ratio.[14] Attempts to obtain [Pt(*O,O′*-acac)$_2$] by treatment of [$PtCl_2(Et_2S)_2$] with K(acac) once again gave, after removal of the chloro ligands with silver perchlorate, [Pt(*O,O′*-acac)(γ-acac)(Et_2S)]. When [$PtCl_2$(S-S)] [S-S = 1,2-bis(ethylthio)ethane] was treated with Tl(acac), [PtCl(γ-acac)(S-S)] was exclusively formed and no other products were obtained even when a large excess of the β-diketonate was used. This latter result clearly indicates that the [PtCl(S-S)]$^+$ moiety prefers to bind to the Cγ-carbon rather than the oxygens of acac. Nevertheless, in the reaction of [$PtCl_2(Et_2S)_2$] with Tl(acac), the isolation of [Pt(*O,O′*-acac)(γ-acac)(Et_2S)] as the only product, without evidence of intermediates, does not explain which of the two coordination modes (*O,O′*-chelated or Cγ-bonded) is preferred when the first acac binds to the metal. It has been suggested that in the reaction of [$PtCl_2(Et_2S)_2$] with acac, the first β-diketonate substitutes one chloro ligand by Cγ-binding to the metal. The second β-diketonate then replaces the other

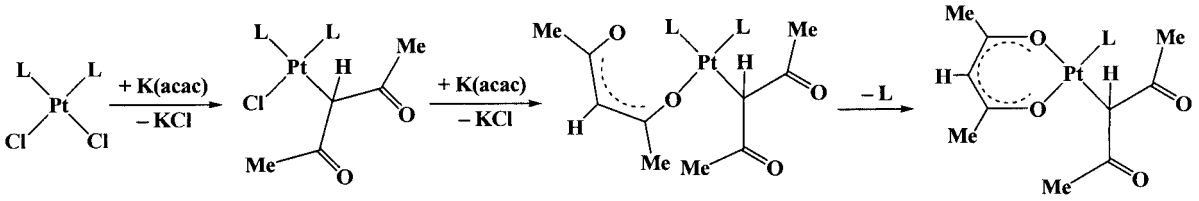

Scheme 4

chloride in a *O*-unidentate mode which finally converts to the *O,O′*-acac chelating mode by sulphide elimination (Scheme 4).

Nevertheless, there is another possible mechanism which cannot be ruled out. According to this mechanism, a cationic β-diketonate chelate first forms, i.e. [Pt(*O,O′*-acac)-$(Et_2S)]^+$, which then bonds to the carbon of the second β-diketonate to give [Pt(*O,O′*-acac)(γ-acac)(Et_2S)] (Scheme 5).[14]

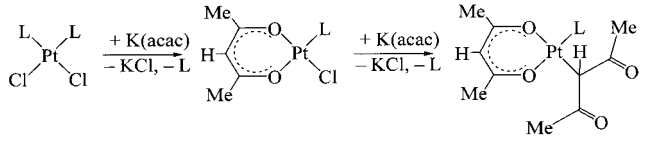

Scheme 5

In this context the synthesis reported here for the **1**, with only the *O,O′*-chelated acac ligand, may be considered important evidence for explaining whether the *O,O′*-chelated or the Cγ σ-bonded acac is the first ligand to coordinate to the metal in the reaction of multiple β-diketonates with platinum. In our investigations, we found that the use of stoichiometric or even substoichiometric amounts of acac with respect to platinum in the reactions with $[PtCl_2(DMSO)_2]$, performed in MeOH, always gave mixtures of **1** and **2**. When we used $K[PtCl_3(DMSO)]$ as a starting complex and water as the solvent, it was possible to exclusively obtain complex **1** which could be isolated in good yield. In principle, the reactivity of $[PtCl_2(DMSO)_2]$ and $K[PtCl_3(DMSO)]$ with chelates can be expected to be very similar.[18] It is well known that both $[PtCl_2(DMSO)_2]$ and $K[PtCl_3(DMSO)]$ react with chelating nitrogen ligands to give the cationic species $[PtCl(DMSO)(N\text{-}N)]^+$ via substitution of one chloride *trans* to DMSO as the first reaction step.[19] In the present case, the formation of a mixture of **1** and **2**, when a suspension of $[PtCl_2(DMSO)_2]$ in MeOH was used in the reaction with acac, can be explained in terms of the low solubility of the starting complex in the reaction medium. In the first step of the reaction, one molecule of acac reacts with the platinum complex to give **1** which is soluble in MeOH and therefore accumulates in the reaction medium. It should be noted that in the formation of compound **1**, as in the formation $[PtCl(DMSO)\text{-}(N\text{-}N)]^+$,[19] the higher *trans* effect of DMSO compared with that of chloride is responsible for both the first attack on platinum by one end of the bidentate ligand and further chelation leading to the thermodynamic product. As the reaction proceeds, complex **2** forms since the second molecule of acac reacts with [PtCl(*O,O′*-acac)(DMSO)] (**1**) rather than with $[PtCl_2(DMSO)_2]$ because of the higher availability of compound **1** in the reaction medium. When we used $K[PtCl_3(DMSO)]$ as the starting complex, [PtCl(*O,O′*-acac)(DMSO)] could be obtained in high yield. In fact **1** is scarcely soluble in water and precipitates from the reaction medium immediately after its formation. It should be noted that **1** could also be obtained by carrying out the reaction of $[PtCl_2(DMSO)_2]$ with a stoichiometric amount of acac in water. In this case, however, a longer reaction time was required due to the much lower solubility of $[PtCl_2\text{-}(DMSO)_2]$ in water compared with that of $K[PtCl_3(DMSO)]$. Finally, further treatment of [Pt(*O,O′*-acac)(γ-acac)(DMSO)] with an extra acac led to the formation of [Pt(*O,O′*-acac)(γ-acac)$_2$]. These results confirm the mechanism depicted in Scheme 5 in which the β-diketonate chelate is the first product formed and the *O,O′*-chelation of the first acac then favours Cγ-carbon bonding of the second (and eventually third) β-diketonate.

Conclusions

In this paper we have described the first two examples of platinum(II) complexes containing both acetylacetonate and sulfoxide ligands coordinated to the metal, namely [PtCl(*O,O′*-acac)(DMSO)] (**1**) and [Pt(*O,O′*-acac)(γ-acac)(DMSO)] (**2**). We have also reported a new synthesis of the homoleptic complex K[Pt(*O,O′*-acac)(γ-acac)$_2$] (**3**).[20] The formation of **2** represents a rare example of a reaction giving [Pt(*O,O′*-acac)(γ-acac)L] complexes starting from platinum species other than [Pt(*O,O′*-acac)$_2$] which also, in general, lack an acac ligand initially bound to the metal. Moreover, the isolation of **1** as an intermediate supports a mechanism in which the β-diketonate chelate is the first product formed from the reaction of multiple β-diketonate ligands with platinum. According to the results reported here, the *O,O′*-chelation of the first acac is followed by the Cγ-carbon bonding of the second (and eventually the third) β-diketonate in the platinum coordination sphere.

Experimental Section

Physical Measurements: Elemental analyses were performed using a Carlo–Erba elemental analyser, model 1106. IR Spectra were recorded with a Perkin–Elmer Spectrum 598 spectrometer using KBr as a solid support for pellets. ^1H and ^{13}C NMR spectra as well as ^1H-^1H NOESY, ^1H-^{13}C HETCOR and ^1H-^{195}Pt HETCOR 2-D experiments were performed with a DPX 400 MHz Avance Bruker instrument using $CDCl_3$, CD_3OD or D_2O as the solvent. Chemical shift are referenced to TMS using the residual protic solvent peaks

as internal references (δ = 7.24 for $CDCl_3$, δ = 3.30 for CD_3OD and δ = 4.65 for D_2O).

Starting Materials: Commercial reagent grade chemicals, acetylacetone and solvents were used without further purification. [Pt(*O,O′*-acac)$_2$],[7] [$PtCl_2(DMSO)_2$][21] and K[$PtCl_3$(DMSO)][22] were prepared by previously reported procedures.

[PtCl(*O,O′*-acac)(DMSO)] (1): A solution of acetylacetone (97.5 mg, 0.973 mmol) and KOH (19.5 mg, 0.487 mmol) in methanol (5 mL) was added dropwise to a solution of K[$PtCl_3$(DMSO)] (204 mg, 0.487 mmol) in water (10 mL) at room temperature with stirring. After few minutes a yellow precipitate separated from the solution. The reaction mixture was left stirring overnight and the pale-yellow precipitate of [PtCl(*O,O′*-acac)(DMSO)] (**1**) was then isolated by filtration and dried under vacuum (yield 149 mg, 75%). $C_7H_{13}ClO_3SPt$ (407.79): calcd. C 20.62, H 3.21; found C 20.73, H 3.28.

Alternatively, a solution containing acetylacetone (97 mg, 0.966 mmol) and KOH (27 mg, 0.483 mmol) in water (5 mL) was added dropwise to a suspension of [$PtCl_2(DMSO)_2$] (204 mg, 0.483 mmol) in water (10 mL) at room temperature with stirring. The reaction mixture slowly became a yellow solution. After 3 h, a pale-yellow solid started to precipitate. The suspension was left stirring for one day and the solid was then filtered and dried under vacuum (yield 27 mg, 26%). $C_7H_{13}ClO_3SPt$ (407.79): calcd. C 20.62, H 3.21; found C 20.51, H 3.18.

[Pt(*O,O′*-acac)(γ-acac)(DMSO)] (2): A solution of acetylacetone (358 mg, 3.576 mmol) and KOH (114 mg, 2.860 mmol) in methanol (5 mL) was added dropwise to a suspension of [$PtCl_2(DMSO)_2$] (302 mg, 0.715 mmol) in methanol (20 mL) at room temperature with stirring. The reaction mixture slowly became a pale yellow solution. After one day, the solvent was evaporated under vacuum and the yellow residue was extracted with $CHCl_3$ (10 mL). The chloroform solution was then filtered to remove KCl and K(acac), pentane (30 mL) was added and the resultant solution kept overnight at 5 °C. Quadrangular pale-yellow crystals of [Pt(*O,O′*-acac)(γ-acac)(DMSO)] (**2**) which separated out from the solution were filtered, washed with pentane and dried under vacuum (yield 168 mg, 50%). $C_{12}H_{20}O_5SPt$ (471.441): calcd. C 30.57, H 4.28; found C 30.73, H 4.34.

K[Pt(*O,O′*-acac)(γ-acac)$_2$] (3): A solution of acetylacetone (332 mg, 3.318 mmol) and KOH (94.8 mg, 2.370 mmol) in methanol (5 mL) was added dropwise to a suspension of [$PtCl_2(DMSO)_2$] (200 mg, 0.474 mmol) in methanol (20 mL) at room temperature with stirring. After 1 h, the suspension became a pale-yellow solution which was left stirring for three days. The solvent was then removed under vacuum and the residual yellow oil was extracted with $CHCl_3$ (10 mL). The chloroform solution was then filtered to separate KCl and K(acac), and pentane (30 mL) was added causing the precipitation of K[Pt(*O,O′*-acac)(γ-acac)$_2$] (**3**) as a yellow solid. The product was separated by filtration, washed with pentane and dried under vacuum (yield 68 mg, 27%). $C_{15}H_{24}KO_6Pt$ (534.524): calcd. C 33.70, H 4.53; found C 33.46, H 4.21.

Alternatively, a solution of acetylacetone (129 mg, 1.284 mmol) and KOH (48 mg, 0.856 mmol) in methanol (10 mL) was added dropwise to a suspension of [Pt(*O,O′*-acac)(γ-acac)(DMSO)] (202 mg, 0.428 mmol) in diethylether (30 mL) at room temperature with stirring. The colour of the solid in the reaction mixture slowly turned from white to pale-yellow. After one day, the solvent was removed under vacuum and the residue was washed with diethyl ether (10 mL) then extracted with chloroform (10 mL). K[Pt(*O,O′*-acac)(γ-acac)$_2$] was obtained as a pale-yellow solid by addition of diethylether (20 mL) to the filtered chloroform solution (yield 65 mg, 28%).

Reaction of [Pt(*O,O′*-acac)$_2$] with DMSO: [Pt(*O,O′*-acac)$_2$] (2 mg, 0.005 mmol), synthesised by a previously reported procedure, was dissolved in $CDCl_3$ (0.5 mL) and the resultant solution placed in an NMR tube. DMSO (1 μL, 1.17 mg, 0.015 mmol) was added and the solution was monitored by recording ^{1}H NMR spectra periodically over a period of two weeks. The spectra did not show any significant change over that period of time.

Single-Crystal X-ray Diffraction Study: Pale-yellow crystals of [Pt(*O,O′*-acac)(γ-acac)(DMSO)] were obtained by crystallisation from $CHCl_3$/pentane. X-ray data were collected using an Enraf–Nonius CAD4 diffractometer. A least-squares algorithm using 25 automatically centred reflections was used to refine the unit cell dimensions. A total of 6726 independent reflections were collected in the range $-10 \le h \le 10$, $-13 \le k \le 14$ and $0 \le l \le 23$. Four reflections were monitored during data collection but no decay was observed. Crystallographic data are summarised in Table 4. The full data set was corrected for Lorentz and polarisation effects and an absorption correction was applied using the DIFABS package[23] at the isotropic stage of refinement. The structure was solved by direct-methods in the $P\bar{1}$ space group. The model was refined by full-matrix least-squares methods. Anisotropic thermal parameters were applied for all non-hydrogen atoms. All hydrogen atoms were placed in their geometrically calculated positions and were included in the full-matrix least-square cycles with isotropic thermal parameters (U) fixed at 1.2 and 1.5 (for methyl group) times the values of *U* of the corresponding carbon atoms. Crystallographic calculations were carried out and molecular graphics designed using the SIR97,[24] SHELXL97,[25] WinGX,[26] ORTEP for Windows[27] and PARST97[28] packages. CCDC-172448 contains the supplementary crystallographic data for this paper. These data can be obtained free of charge from The Cambridge Crystallographic Data Centre via www.ccdc.cam.ac.uk/data_request/cif.

Supporting Information (see footnote on the first page of this article): Figure S1, ^{1}H-^{13}C HETCOR and long range HETCOR NMR spectra of **1**. Figures S2, molecular structure of *2a*. Figure S3, molecular structure of *2b*. Figure S4, unit cell projection of **2** along *a*-axis with all atoms except hydrogens. Table S5, anisotropic displacement parameters for *2* and *2a*. Table S6, anisotropic displacement parameters for *2b*.

Acknowledgments

The authors gratefully acknowledge Mr. Alessandro Laurita (University of Potenza) for the X-ray diffraction data collection. This work was supported by the University of Lecce and the Ministero dell'Istruzione, dell'Università e della Ricerca (M.I.U.R.), Cofin. 2003 (No. 2003039774_005).

[1] F. P. Fanizzi, G. Natile, M. Lanfranchi, A. Tiripicchio, *Inorg. Chim. Acta* **1997**, *264*, 11–18.
[2] M. Calligaris, O. Carugo, *Coord. Chem. Rev.* **1996**, *153*, 83–154.
[3] D. A. Thomton, *Coord. Chem. Rev.* **1990**, *104*, 173–249.
[4] S. Gama de Almeida, J. L. Hubbard, N. Farrell, *Inorg. Chim. Acta* **1992**, *193*, 149–157.
[5] A. Werner, *Ber. Dtsch. Chem. Ges.* **1901**, *34*, 2584.
[6] Lewis, Long, Oldham, *J. Chem. Soc.* **1965**, 6740–6747.
[7] G. T. Behnke, K. Nakamoto, *Inorg. Chem.* **1967**, *6*, 433–440.
[8] G. T. Behnke, K. Nakamoto, *Inorg. Chem.* **1967**, *6*, 440–445.
[9] G. T. Behnke, K. Nakamoto, *Inorg. Chem.* **1968**, *7*, 330–338.

[10] S.Okeya, Y. Nakamura, S. Kawaguchi, *Bull. Chem. Soc. Jpn.* **1982**, *55*, 1460–1466.
[11] S. Baba, T. Ogura, S. Kawaguchi, *Bull. Chem. Soc. Jpn.* **1974**, *47*, 665–668.
[12] T. Ito, T. Kiriyama, A. Yamamoto, *Bull. Chem. Soc. Jpn.* **1976**, *49*, 3250–3256.
[13] T. Ito, T. Kiriyama, Y. Nakamura, A. Yamamoto, *Bull. Chem. Soc. Jpn.* **1976**, *49*, 3257–3264.
[14] F. Sasakura, K. Isobe, S. Kawaguchi, *Bull. Chem. Soc. Jpn.* **1985**, *58*, 657–663.
[15] L. Carlton, *Relative Sign of J Couplings from Two-Dimensional NMR Spectra*, *Bruker Report* **2000**, no. 148, p. 28–29.
[16] R. Mason, G. B. Robertson, *J. Chem. Soc. A* **1969**, 485–492.
[17] K. J. Cavell, H. Jin, B. W. Skelton, A. H. White, *J. Chem. Soc. Dalton Trans.* **1993**, 1973–1978.
[18] P. Kong, D. Iyamuremye, F. D. Rochon, *Bioinorganic Chemistry* **1976**, *6*, 83–89.
[19] N. Farrell, S. Gama de Almeida, Y. Qu, *Inorg. Chim. Acta* **1990**, *178*, 209–211.
[20] T. Ito, T. Kiriyama, Y. Nakamura, A. Yamamoto, *Bull. Chem. Soc. Jpn.* **1976**, *49*, 3257–3264.
[21] Yu. N. Kukushkin, Yu. E. Vyaz'menskii, L. I. Zorina, Yu. L. Pazukhina, *Russian J. Inorg. Chem. (Engl. Transl.)* **1968**, *13*, 835–838.
[22] Yu. N. Kukushkin, Yu. E. Vyaz'menskii, L. I. Zorina, *Russian J. Inorg. Chem. (Engl. Transl.)* **1968**, *13*, 1573–1576.
[23] N. Walker, D. Stuart, *Acta Crystallogr., Sect. A* **1983**, *39*, 158–166.
[24] A. Altomare, M. C. Burla, M. Camalli, G. L. Cascarano, C. Giacovazzo, A. Guagliardi, A. G. G. Moliterno, G. Polidoro, R. Spagna, *SIR97*, *A program for automatic solution and refinement of crystal structures*, **1996**.
[25] G. M. Sheldrick, *SHELXL97*, *Program for the refinement of crystal structures*, University of Göttingen, Germany, **1997**.
[26] *An Integrated System of Windows Programs for the Solution, Refinement and Analysis of Single Crystal X-ray Diffraction Data*, L. J. Farrugia *J. Appl. Cryst.* **1999**, *32*, 837–838.
[27] *ORTEP-3 for Windows – A Version of ORTEP-III with a Graphical User Interface (GUI)*, L. J. Farrugia, *J. Appl. Cryst.* **1997**, *30*, 565.
[28] M. Nardelli, *PARST 97, A System of Computer Routines for Calculating Molecular Parameters from the Results of Crystal Structure Analysis*, University of Parma, Italy, **1996**.

Received: July 29, 2004
Published Online January 27, 2005

